Response of terrestrial ecosystems to recent Northern Hemispheric drought

Alexander Lotsch,[1] Mark A. Friedl,[2] Bruce T. Anderson,[2] and Compton J. Tucker[3]

Received 19 November 2004; revised 17 January 2005; accepted 11 February 2005; published 19 March 2005.

[1] Satellite normalized difference vegetation index (NDVI) observations reveal large and geographically extensive decreases in vegetation activity in Eurasia and North America between 1999 and 2002. In 2001, 73% of central southwest Asia exhibited NDVI anomalies that were more than one standard deviation below 21-year average conditions, and in 2002, fully 95% of North America exhibited below-average NDVI. This episode of large-scale vegetation browning coincided with a prolonged period of below-normal precipitation in the Northern Hemisphere, which limited moisture availability for plant growth. Spatio-temporal dynamics of NDVI, precipitation, and sea surface temperature data reveal that synchronous patterns of ocean circulation anomalies in the Pacific, Atlantic, and Indo-Pacific are strongly correlated with observed joint variability in NDVI and precipitation in the Northern Hemisphere during this period. **Citation:** Lotsch, A., M. A. Friedl, B. T. Anderson, and C. J. Tucker (2005), Response of terrestrial ecosystems to recent Northern Hemispheric drought, *Geophys. Res. Lett.*, *32*, L06705, doi:10.1029/2004GL022043.

1. Introduction

[2] Improved knowledge of ecosystem response to climate variability is important to understand changes in spatio-temporal patterns of biosphere-atmosphere interactions that may arise from climate changes, including fluxes of carbon, water and energy [*Bonan*, 2002]. In particular, future climate perturbations are likely to result in substantial changes, both globally and locally, to precipitation regimes [*Intergovernmental Panel on Climate Change*, 2001; *Trenberth et al.*, 2003], and may therefore alter exchange processes at the biosphere-atmosphere interface.

[3] Terrestrial ecosystems show significant response to inter-annual fluctuations in precipitation patterns associated with perturbations in the ocean-atmosphere circulation system [*Nemani et al.*, 2003]. Specifically, global climate in recent years was characterized by a period of geographically extensive and prolonged drought episodes in the Northern Hemisphere, which limited moisture availability for plant growth, and affected primarily central southwest (CSW) Asia [*Barlow et al.*, 2002] and North America [*Hoerling and Kumar*, 2003]. Because of the potential sensitivity of the global hydrologic cycle to climate change, this period of extreme drought provides a unique natural experiment to help scientists understand how perturbations in the ocean-atmosphere system affect terrestrial ecosystems, and by extension, agricultural production and food security of entire countries.

[4] At global scales the response of vegetation to climate perturbations has been widely observed using satellite-based measurements of normalized difference vegetation index (NDVI) [*Lucht et al.*, 2002], which is proportional to the amount of photosynthetically active radiation absorbed by vegetation [*Asrar et al.*, 1984] and indicative of terrestrial ecosystem productivity [*Myneni et al.*, 1995; *Tucker*, 1979].

[5] We hypothesized that observed patterns of reduced plant growth between 1999 and 2002 were related to a recent hemispheric-scale drought caused by anomalies in global sea surface temperatures (SST). To test this hypothesis, we examined (1) spatio-temporal correlation between 1981–2002 NDVI time series produced from National Oceanic and Atmospheric Administration (NOAA) Advanced Very High Resolution Radiometer (AVHRR) data and global precipitation, and (2) the link of principal modes of precipitation variability with SSTs.

2. Data and Methods

2.1. NDVI

[6] The raw NOAA-AVHRR sensor data at 8-km spatial and 15-day temporal resolution has been reprocessed by the National Aeronautics and Space Administration (NASA) Global Inventory Monitoring and Modeling Studies (GIMMS) group to provide a spatially and temporally consistent representation of global vegetation for climate studies, and to remove effects associated with calibration changes, orbital drift and aerosol contamination of the atmosphere [*Tucker et al.*, 2004]. For this study, the data was aggregated to 1 degree spatial and 1 month temporal resolution to minimize the effect of spatial and temporal autocorrelation. Anomalies were calculated relative to 1981–2002 June–August (JJA) means and normalized by the standard deviation estimated from 21 seasonal observations for the same season.

2.2. Precipitation

[7] The precipitation time series used in this analysis are based on monthly land observations from weather stations included in the Global Historical Climatology Network and the Climate Anomaly Monitoring System spanning the period from 1948 to 2002 [*Chen et al.*, 2002].

[8] To investigate how recent changes in plant growth are related to spatial and temporal patterns of precipitation we constructed time series of the standardized precipitation index (SPI) based on monthly observations of precipitation

[1]Development Research Group, The World Bank, Washington, D. C., USA.
[2]Center for Remote Sensing, Department of Geography, Boston University, Boston, Massachusetts, USA.
[3]Biospheric Sciences Branch, NASA Goddard Space Flight Center, Greenbelt, Maryland, USA.

0094-8276/05/2004GL022043

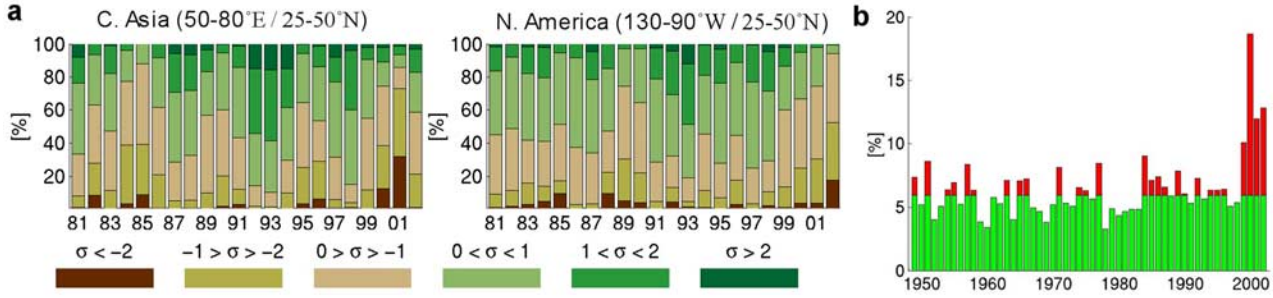

Figure 1. (a) Fractional land area showing NDVI deviations from 1981–2002 mean conditions. Fractional land area (in percent) is shown as positive (green) and negative (brown) standardized departures (σ) of NDVI from the 1981–2002 (x-axis) summer (July–August) mean. This graph summarizes anomalies for CSW Asia (50°–80°E, 25°–50°N; left panel) and western North America (130°–90°W, 25°–50°N; right panel). Anomalies were binned into moderate ($0 \leq |\sigma| < 1$), strong ($1 \leq |\sigma| < 2$) and extreme ($2 \leq |\sigma|$) deviations from the mean. Particularly extreme reductions in vegetation greenness (dark brown) occurred in 2001 in central southwest Asia and in 2002 in western North America. (b) Northern Hemispheric (20°–50°N) fractional land area affected by severe seasonal drought (1948–2002). Severe seasonal drought is defined as 6-month SPI values smaller than −1.5. The red portion of the bars indicates above average fractional area of severe droughts for the period from 1948–2002. Annually (October–September) averaged percentage of land area affected by severe drought increases sharply from a multi-decadal average of 5–10% to nearly 19% in 2000.

[*McKee et al.*, 1993]. This index captures the accumulated deficit (SPI < 0) or surplus (SPI > 0) of precipitation over a specified period of time and provides a normalized measure (i.e. spatially invariant Z score) of relative precipitation anomalies at multiple time scales. Because the SPI is normalized using climatological mean values, it is equally effective at representing dry and wet anomalies. For this study, a 6-months time scale was chosen based on previous analyses of NDVI-SPI covariability [*Lotsch et al.*, 2003].

2.3. SSTs

[9] To investigate inter-annual fluctuations in SSTs, data from the National Center for Environmental Prediction (NCEP) reanalysis are used [*Kalnay et al.*, 1996]. This data is used to characterize the leading modes of SST variability in each ocean basin according to well-known patterns of ocean-atmosphere interactions.

3. Results

[10] Figure 1a shows JJA standard deviations (σ) from NDVI for mid-latitudes in North America and CSW Asia for 1981–2002 expressed as the spatially averaged fraction of total land area. CSW Asia (left panel) shows pronounced year-to-year variability with a 4–5 year cycle and exhibits significant negative departures from mean NDVI (olive to dark brown colours) in 1999–2001. Most notably, 2001 shows the largest anomaly for the 21-year period, with nearly 40% and 33% of CSW Asia having strong ($-2 < \sigma < -1$) and extreme ($\sigma < -2$) deviations from the mean, respectively, and reflecting the significant deficit in rainfall during this period [*Barlow et al.*, 2002]. Similarly, an increase in the area of below-normal NDVI patterns was observed for western North America (middle panel) in 1999–2002, with 95% of land area exhibiting below average NDVI values in 2002 (33% with $-2 < \sigma < -1$ and 18% with $\sigma < -2$). This level of browning is unparalleled in the 21-year NDVI record. Northern Hemisphere maps of JJA NDVI anomalies for 1998, 2001 and 2002 are shown in Figure 2 and illustrate the geographic extent of areas in the Northern Hemisphere that were affected by reduced plant activity.

[11] To appreciate the magnitude and extent of this recent drought relative to precipitation regimes over the past 55 years, Figure 1b presents the proportion of land area affected by severe drought (SPI < −1.5) for the Northern Hemisphere mid-latitudes (20–50°N) between 1948 and 2002, which clearly captures the pronounced deficits in precipitation between 1999–2002. Notably, while the percentage of severely drought-affected land area ranged between 5 and 10% for the period between 1948 and the mid-1990s, up to 19% of Northern Hemisphere land areas experienced severe drought between 1999 and 2002.

[12] The close linkage between spatio-temporal variability in precipitation and vegetation is further illustrated in Figure 3 by the leading joint mode obtained from pattern-based analysis for Eurasia for 1981–2003. Specifically, year-to-year fluctuations (right) in NDVI are highly correlated with changes in SPI and are particularly pronounced in areas affected by the recent (1999–2002) drought episode

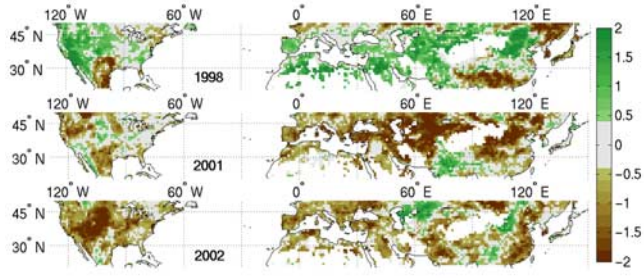

Figure 2. Summer NDVI anomalies for 1998, 2001 and 2002. Northern Hemisphere mid-latitude summer (July–August) anomalies of NDVI are indicative of ecosystem photosynthetic activity. Brown colours indicate negative standard deviations from 1981–2002 July–August means, and positive deviations are shown in green.

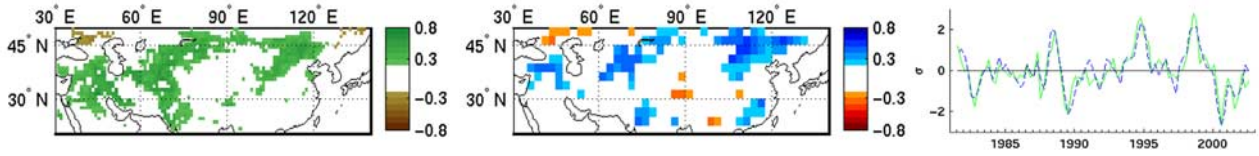

Figure 3. Leading mode of NDVI-SPI covariability for Eurasia (1981–2003). Patterns were estimated using canonical correlation analysis [*Bretherton et al.*, 1992], which estimates principal modes of joint variability from two multivariate datasets. Normalized ($\sigma = 1$) year-to-year covariability (right) of NDVI (green line) and 6-month SPI (blue line) is high ($r = 0.8$). Statistically significant spatial correlations ($|r| > .2$; $p = .05$) for NDVI (left) and SPI (centre) correspond to the respective time series in the right panel. High degree of spatial coincidence indicates precipitation-induced changes in vegetation.

(left: NDVI, centre: SPI; see caption for details). Similar patterns of NDVI-SPI covariability were identified for other regions in *Lotsch et al.* [2003].

[13] Prior modelling studies have shown that a protracted phase of cold eastern Pacific SSTs (La Niña) and warming in the Indo-Pacific from 1998–2002 provided a key mechanism leading to widespread Northern Hemispheric drought [*Hoerling and Kumar*, 2003]. However, our empirical analyses suggest that ocean-atmosphere dynamics outside of the tropical Pacific also contribute strongly to observed SPI and NDVI anomalies and need to be considered to fully explain the spatial extent and magnitude of the observed drought patterns. To assess these contributions, we examined the relationship between ocean-atmosphere circulation processes in the Pacific, Atlantic, and Indian Oceans and precipitation anomalies over adjacent land masses. That is, to characterize temporal patterns in precipitation regimes at continental scales, leading principal components (PC) were estimated for Northern Hemisphere 1948–2002 time series of 6-month SPI in America (160°–50°W), Europe and Africa (30°W–80°E), and Eurasia (60°–160°E).

[14] The PC time series are shown as standardized anomalies in Figure 4 (lines in top panels), and exhibit high temporal correlation with widely used indices of ocean-atmosphere interaction in different ocean basins (shown as blue/red bars). The maps in the bottom panels show the spatial manifestation of the PC time series and illustrate the spatial coincidence between the regions experiencing strong NDVI-SPI covariability (Figures 2 and 3).

[15] More specifically, the Pacific Decadal Oscillation (PDO) is a multi-decadal mode of low-frequency variability in SSTs in the Pacific Ocean (north of 20°N), and has been shown to influence remote precipitation regimes in the Western Hemisphere [*Mantua et al.*, 1997]. For the Amer-

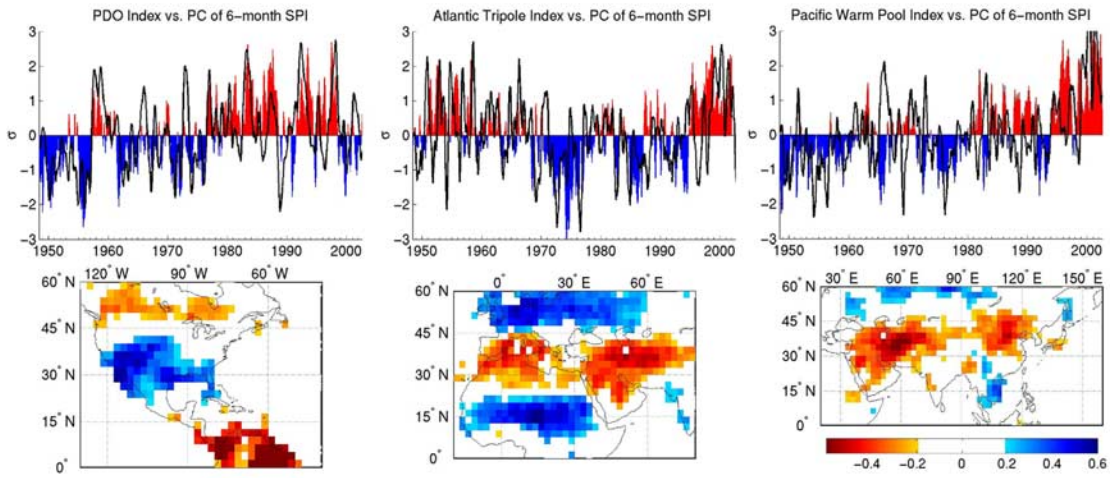

Figure 4. Empirical ocean-drought linkages for Northern Hemisphere land area. Top panels show standardized principal components (black lines) estimated from seasonal 1948–2002 6-month SPI time series for the Northern Hemisphere in America (160°–50°W), Europe and Africa (30°W–60°E), and Eurasia (60°–160°E). The temporal patterns capture interannual variability of dry and wet anomalies at continental scales. Spatial associations are shown in the bottom panels, where blue/red colours indicate significant ($r > |.2|$; $p = .01$) positive/negative correlations (component loadings). For reference, time series of the PDO, ATP, and PWA are shown as positive (red) and negative (blue) departures from the 1948 to 2002 mean in each panel. These ocean indices are defined as the leading spatial modes of Pacific, Atlantic and Indo-Pacific seasonal SST anomalies and characterize slow forcing of associated atmospheric circulation patterns. The principal component time series show strong seasonal correlation with the PDO ($r = 0.64$) in February–April, the ATP ($r = 0.54$) in May–July, and the PWA ($r = 0.48$) in March–May. Note that the lag in the relationship between summer (JJA) SPI and antecedent changes in ocean-atmosphere circulation arises from the fact that the SPI integrates precipitation over the 6-month period leading up to the JJA season.

ican sector (160°–50°W) such teleconnections are reflected in the leading mode of SPI variability, which captures higher frequency variability associated with the El Niño Southern Oscillation (ENSO) superimposed on lower frequency variability associated with the PDO. This component explains 55% of the temporal variance in SPI (left panels). Note that the PDO was in a positive phase for most of the 1980s and 1990s, but recently exhibited a significant cold (negative) episode that coincided with anomalously cold SSTs during 1998–2002. Constructive phasing of ENSO and PDO is known to enhance ENSO teleconnections in North America, whereas destructive phasing tends to weaken these linkages [*Gershunov and Barnett*, 1998]. Thus, the confluence of negative phases for both the PDO and ENSO contributed to strong precipitation deficits (and hence NDVI anomalies) in North America during 1998–2002.

[16] SPI variability between 30°W–80°E is characterized by a tripole pattern with latitudinally alternating anomalies over northern Europe, the Mediterranean (extending into the middle East and CSW Asia), and the northern Sahel. This variability is captured by the leading PC of SPI (middle panels). During positive (negative) departures, dry (wet) conditions prevail in the Mediterranean and CSW Asia, whereas northern Europe and the Sahel tend to be wetter (drier) than normal. These patterns are correlated with the Atlantic Tripole (ATP) [*Deser and Timlin*, 1997], which is a well-defined mode of low-frequency fluctuations in Atlantic SSTs (10–70°N, 0–80°W) and is associated with atmospheric circulation that causes changes in precipitation similar to the patterns observed in SPI [*Visbeck et al.*, 2001; *Thompson and Wallace*, 2000].

[17] For Eurasia (60–160°E) the first PC reveals a mode of variability that is characterized by a positive trend associated with decreasing (drier) SPI in CSW and northeastern Asia over the past 20 years (right panels of Figure 4). Particularly strong positive anomalies have occurred since the mid-nineties and are related to extreme below-normal winter precipitation, which is reflected in summer SPI values. Droughts in this region are related in part to large-scale upper-level atmospheric circulation patterns induced by strong latent heat release in the Indo-Pacific [*Barlow et al.*, 2002]. The latent heat anomaly is embedded in a multi-decadal warming trend of SSTs in the Pacific Warm Pool (PWA) region (60–170°E, 15°S–15°N), which exhibited a rate of warming during the 1998–2002 La Niña event that was unprecedented in the 20th century (Figure 4).

4. Conclusions

[18] The results presented in this paper reveal strong empirical evidence of joint variability in the ocean-atmosphere-biosphere system. It is becoming increasingly evident that large-scale perturbations of the terrestrial biosphere such as those described here can propagate into other components of the climate system, with important implications for the direction and magnitude of biosphere-atmosphere fluxes of water and carbon [*Prentice and Fung*, 1990; *Koster et al.*, 2000]. Globally, dry and warm conditions are associated with a net release of carbon, whereas wet and cool years tend to increase terrestrial carbon uptake [*Schimel et al.*, 2001]. While increases in growing season temperatures have caused increased carbon uptake by boreal forests [*Myneni et al.*, 2001], warmer temperatures associated with precipitation deficits have negative consequences for plant growth, especially in semi-arid ecosystems such as those affected by the 1998–2002 drought. Positive trends in precipitation associated with warmer temperatures, on the other hand, will tend to increase ecosystem productivity and can result in terrestrial carbon uptake [*Nemani et al.*, 2002]. Finally, a variety of recent evidence suggests that land-atmosphere coupling [*Deser and Timlin*, 1997; *Pielke et al.*, 1998] provides an important positive feedback within the climate system, which can lead to catastrophic droughts such as the one experienced in the Great Plains of North America in the 1930's [*Schubert et al.*, 2004]. Indeed, such feedback mechanisms may explain much of the variance in precipitation and NDVI that is not accounted for by SST anomalies in this work.

[19] In conclusion, the recently observed patterns of below-normal NDVI reveal terrestrial ecosystem dynamics that are strongly correlated with unique and synchronous ocean-atmosphere fluctuations in the Pacific, Atlantic, and Indo-Pacific. Because spatial and temporal patterns in global precipitation regimes are expected to change as a consequence of an intensified global hydrological cycle, a better understanding of the causal mechanisms and effects of such droughts on global ecosystems and society is important for appropriate climate change policy formulation.

[20] **Acknowledgments.** We thank Jorge Pinzón for help in the calibration of the GIMMS NDVI data. This work was supported by the NASA Intelligent Data Understanding Program, Grant NCC2-1245.

References

Asrar, G., et al. (1984), Estimating absorbed photosynthetic radiation and leaf area index from spectral reflectance in wheat, *Agron. J.*, *76*, 300–306.

Barlow, M., et al. (2002), Drought in central and southwest Asia: La Niña, the warm pool, and the Indian Ocean precipitation, *J. Clim.*, *15*, 697–700.

Bonan, G. (2002), *Ecological Climatology: Concepts and Applications*, Cambridge Univ. Press, New York.

Bretherton, C. S., et al. (1992), An intercomparison of methods for finding coupled patterns in climate data, *J. Clim.*, *5*, 541–560.

Chen, M., et al. (2002), Global land precipitation: A 50-year monthly analysis based on gauge observations, *J. Hydrometeorol.*, *3*, 249–266.

Deser, C., and M. S. Timlin (1997), Atmosphere-ocean interaction on weekly timescales in the North Atlantic and Pacific, *J. Clim.*, *10*, 393–408.

Gershunov, A., and T. P. Barnett (1998), Interdecadal modulation of ENSO teleconnections, *Bull. Am. Meteorol. Soc.*, *79*, 2715–2725.

Hoerling, M., and A. Kumar (2003), The perfect ocean for drought, *Science*, *299*, 691–694.

Intergovernmental Panel on Climate Change (2001), *Climate Change 2001: The Scientific Basis*, edited by J. T. Houghton et al., Cambridge Univ. Press, New York.

Kalnay, E., et al. (1996), The NCEP/NCAR 40-year reanalysis project, *Bull. Am. Meteorol. Soc.*, *77*, 437–470.

Koster, R. D., et al. (2000), Variance and predictability of precipitation at seasonal-to-interannual timescales, *J. Hydrometeorol.*, *1*, 26–46.

Lotsch, A., M. A. Friedl, B. T. Anderson, and C. J. Tucker (2003), Coupled vegetation-precipitation variability observed from satellite and climate records, *Geophys. Res. Lett.*, *30*(14), 1774, doi:10.1029/2003GL017506.

Lucht, W., et al. (2002), Climatic control of the high-latitude vegetation greening trend and Pinatubo effect, *Science*, *296*, 1687–1689.

Mantua, N. J., et al. (1997), A Pacific interdecadal climate oscillation with impact on salmon production, *Bull. Am. Meteorol. Soc.*, *78*, 1069–1079.

McKee, T., et al. (1993), The relationship of drought frequency and duration to time scales, paper presented at 8th Conference on Applied Climatology, Am. Meteorol. Soc., Boston, Mass., 17–22 Jan.

Myneni, R. B., et al. (1995), The interpretation of spectral vegetation indexes, *IEEE Trans. Geosci. Remote Sens.*, *33*, 481–486.

Myneni, R. B., et al. (2001), A large carbon sink in the woody biomass of northern forests, *Proc. Natl. Acad. Sci. U. S. A.*, *98*, 14,784–14,789.

Nemani, R., M. White, P. Thornton, K. Nishida, S. Reddy, J. Jenkins, and S. Running (2002), Recent trends in hydrologic balance have enhanced the terrestrial carbon sink in the United States, *Geophys. Res. Lett.*, *29*(10), 1468, doi:10.1029/2002GL014867.

Nemani, R., et al. (2003), Climate-driven increases in global terrestrial net primary production from 1982 to 1999, *Science*, *300*, 1560–1563.

Pielke, R. A., et al. (1998), Interactions between the atmosphere and terrestrial ecosystems: Influence on weather and climate, *Global Change Biol.*, *4*, 461–475.

Prentice, K. C., and I. Y. Fung (1990), The sensitivity of terrestrial carbon storage to climate change, *Nature*, *346*, 48–51.

Schimel, D., et al. (2001), Recent patterns and mechanisms of carbon exchange by terrestrial ecosystems, *Nature*, *414*, 169–172.

Schubert, S. D., et al. (2004), On the cause of the 1930's dust bowl, *Science*, *303*, 1855–1859.

Thompson, D. W. J., and J. M. Wallace (2000), Annular modes in the extratropical circulation. Part II: Trends, *J. Clim.*, *13*, 1018–1036.

Trenberth, K. E., et al. (2003), The changing character of precipitation, *Bull. Am. Meteorol. Soc.*, *84*, 1205–1217.

Tucker, C. J. (1979), Red and photographic infrared linear combinations for monitoring vegetation, *Remote Sens. Environ.*, *8*, 127–150.

Tucker, C. J., et al. (2004), An extended AVHRR 8-km NDVI data set compatible with MODIS and SPOT vegetation NDVI data, *Int. J. Remote Sens.*, in press.

Visbeck, M. H., et al. (2001), The North Atlantic Oscillation: Past, present, and future, *Proc. Natl. Acad. Sci. U. S. A.*, *98*, 12,876–12,877.

B. T. Anderson and M. A. Friedl, Center for Remote Sensing, Department of Geography, Boston University, 675 Commonwealth Ave., Boston, MA 02215-1401, USA. (friedl@bu.edu; brucea@bu.edu)

A. Lotsch, Development Research Group, The World Bank, 1818 H Street NW, Washington, DC 20433, USA. (alotsch@worldbank. org)

C. J. Tucker, Biospheric Sciences Branch, NASA Goddard Space Flight Center, Greenbelt, MD 20771, USA. (compton@ltpmailx.gsfc.nasa.org)